Supplementary information for

Designing an S-scheme heterojunction based on MOF-808-NH_2 and TpTt-COF for enhanced photocatalytic performance of alkylphenols under visible light

Haiyue Yuan[a], Jianhui Zhu[b], Desheng Liu[a], Mengyao Wang[a], Siyue Zhu[a], Xinping Hu[a], Yongqiang Ma[a*], Yan Wang[c*]

[a] Department of Applied Chemistry, College of Science, China Agricultural University, Beijing, 100193, P.R. China

[b] College of Resources and Environmental Sciences, China Agricultural University, Beijing, 100193, China

[c] Institute of Environment and Sustainable Development in Agriculture, Chinese Academy of Agricultural Sciences

* Corresponding author:

1. Yongqiang Ma, Department of Applied Chemistry, College of Science, China Agricultural University, Yuanmingyuan West Road No.2, Haidian District, Beijing, 100193, P.R. China

E-mail address: mayongqiang@cau.edu.cn

2. Yan Wang, Institute of Environment and Sustainable Development in Agriculture, Chinese Academy of Agricultural Sciences, Beijing 100081, China

E-mail address: wangyan03@caas.cn

Experimental Section

Materials and methods

Chemicals and reagents. 4-Butylpheno (4-BP), 4-Pentylphenol (4-PP), 4-Heptylphenol (4-HP), 4-tert-Octylphenol (4-t-OP), 4-Octylphenol (4-OP), 4-Nonylphenol (4-NP), 2,4,6-Trihydroxy-benzene-1,3,5-tricarbaldehyde (Tp), N-N-Dimethylacetamide (DMAc), Zirconyl chloride octahydrate ($ZrOCl_2 \cdot 8H_2O$), 5-aminoisophthalic acid, Dimethyl sulfoxide (DMSO), Fulvic acid, p-phthalic acid (PTA), and ethyl acetate (HPLC grade) were obtain from MREDA, Beijing, Technology Co., Ltd. Formic acid (FA), Acetic Acid (AA), Sodium chloride (NaCl), Sodium sulfate (Na_2SO_4), Magnesium chloride ($MgCl_2$), Potassium chloride (KCl), Ferric chloride ($FeCl_3$), Calcium chloride ($CaCl_2$), Sodium carbonate (Na_2CO_3), Sodium bicarbonate ($NaHCO_3$), Sodium dihydrogen phosphate (NaH_2PO_4), Fulvic acid, tert-Butanol (*t*-Bu), Potassium bromate ($KBrO_3$), 1,4-Benzoquinone (*p*-BQ) and Isopropanol were purchased from Energy Chemistry, Anhui Zesheng, Technology Co., Ltd. N,N-Dimethylformamide (DMF), Melamine (Tt), ethyl alcohol, acetone, Edetate disodium (EDTA-2Na), Sodium hydroxide (NaOH), Hydrochloric acid (HCl, 36 %) were purchased from the Chinese Sinopharm Chemical Reagent Co., Ltd. (Shanghai, China). All chemicals were of analytical grade or higher grade and used directly without purification.

Photocatalytic experiments. The photocatalytic degradation experiments were carried out under Xe lamp irradiation with a cut-off filter (300 W, Light intensity= 100 mW cm^2, $\lambda > 400$ nm). 5 mg photocatalyst was added to 50 mL of APs (4-BP, 4-PP, 4-HP, 4-t-OP, 4-OP, 4-NP) solution (1 $mg \cdot L^{-1}$) and the suspension was stirred in the dark for 30 min before irradiation. Then the Xe lamp was turned on and 1 mL of the suspension was extracted at specific time intervals (20, 40, 60, 80, 100 and 120 min). The samples were subjected to liquid-liquid extraction using ethyl acetate and then analyzed by Agilent 7890A gas chromatograph, coupled with a 7000C triple-quadrupole mass spectrometer (SIM model). Sodium hydroxide and hydrochloric acid were used to investigate the effect of pH, while chloride salts and sodium salts were used to explore the effects of different anions and cations. EDTA-2Na, t-Bu, $KBrO_3$, p-BQ were used as scavengers for holes (h^+), hydroxyl radicals ($\cdot OH$), electrons (e^-) and superoxide radicals ($\cdot O_2^-$) in the scavenging experiments, respectively. Degradation intermediates were also identified by GC-MS/MS (Agilent 7890A, Full scan model). The detailed instrument parameter was described in the Supplementary Material Table S1.

Photocatalytic characterization: Microstructural features images of the photocatalysts were obtained using a scanning electron microscope (SEM, SU8020) and transmission electron microscopy (TEM, FEI Tecnai G2 F30). The crystalline phase of the material was determined using an X-ray diffractometer (XRD, D8 ADVANCE) with CoKα as the radiation source at 40mA and 40kV (λ=1.79026 Å). The scan rate was set to 5°/min, with a scanning range from 5° to 50°. The light absorption properties of the catalytic material were measured by UV-visible absorption spectroscopy (UV-3600, SHIMADZU, Japan) over a wavelength range of 200-800 nm. Fourier-transform infrared (FT-IR) spectra were recorded using a Nicolet 6700 FT-IR spectrometer with a wavenumber range of 400-4000 cm^{-1}. Pore size and Brunauer-Emmett-Teller (BET) specific surface area were obtained using ASAP 2460 (Micromeritics, USA). X-ray photoelectron spectroscopy (XPS, Thermo Escalab 250XI) with single Al-Kα at 150W was used to further investigate the structure and chemical states of the material. The photoluminescence (PL) spectroscopy and fluorescence lifetime of the catalyst were collected using an FLS980 (Edinburgh Instruments Ltd.). Electrochemical tests were performed using a CHI-700D ectrochemical working station. Pt wire, Ag/AgCl (saturated KCl) and ITO glass electrode were as the counter electrode, reference electrode and the working electrode, respectively. A 300 W Xe lamp with a 400 nm filter simulated the visible light irradiation and was switched every 20 s for the photocurrent test. Electrochemical Impedance Spectroscopy (EIS) was conducted in the frequency range of 0.1 to 100000 Hz. And the frequency range of Mott-Schottky curve (M-S) were 1000Hz and 2000Hz. The zeta potential (mV) of the catalyst was measured at different pH levels using a Zetasizer Nano ZS90. Electron paramagnetic resonance (EPR, A300-10/12, Bruker) was utilized to further determine the types of free radicals generated by the hybrid material at room temperature under visible light irradiation (The detailed experimental steps are as 'ESR experiment' section). Thermogravimetric analysis (TGA, NETZSCH STA2500, Germany) was employed to assess the thermal stability of the material. Total organic carbon (TOC, MULTI N/C® 2100, Germany) analysis was conducted to measure the total organic carbon in the degraded aqueous solution, which reflects the extent of mineralization.

ESR experiment

Hydroxyl Radicals: A 1 $mg\cdot mL^{-1}$ sample aqueous solution was prepared and dispersed. Then, 100 μL of this solution was mixed with 100 μL of a 100 mM DMPO solution.

Superoxide Radicals: A 1 $mg\cdot mL^{-1}$ sample methanol solution was prepared and dispersed. Then, 100 μL of this solution was mixed with 100 μL of a 100 mM DMPO solution.

Photogenerated Holes: A 1 mg·mL^{-1} sample aqueous solution was prepared and dispersed. Then, 100 μL of this solution was mixed with 100 μL of a 20 mM TEMPO solution.

The mixture was then transferred into a capillary tube, sealed, and placed into a sample holder for data collection under both dark and light conditions for 10 minutes, using a 300W Xenon lamp.

Toxicity predicted. This work was supported by the Toxicity Estimation Software Tool (T.E.S.T, Version 5.1, US EPA) to evaluate the developmental toxicity of degradation intermediates. Additionally, the ECOSAR tool (Version 2.2, US EPA) is one of the best programs for predicting aquatic toxicity [1]. It provided 96-hour LC50 and EC50 results for parent compounds and degradation products in aquatic organisms (fish and green algae), thereby enabling the assessment of ecological toxicity risks.

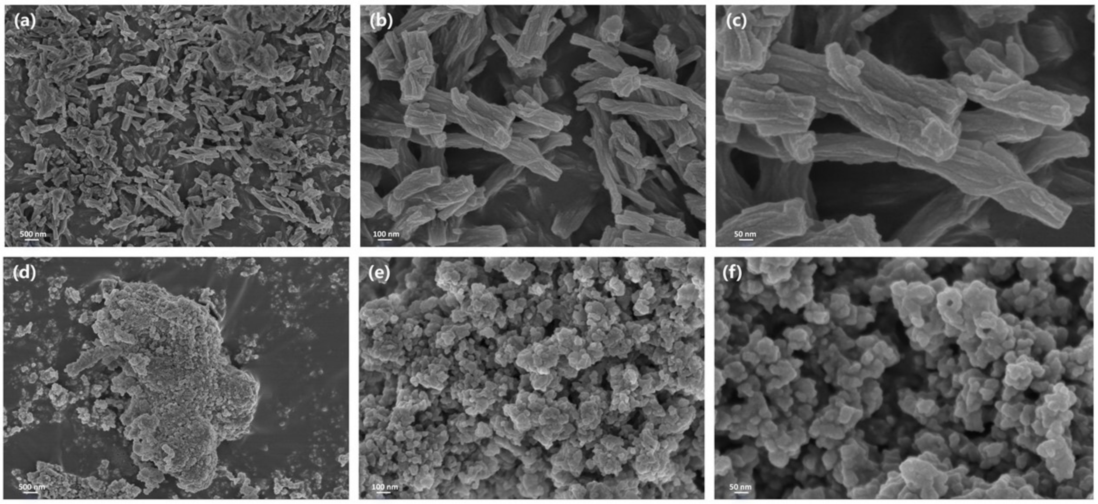

Fig. S1 SEM images of Zr-MOF (a-c) and TpTt-COF (d-f)

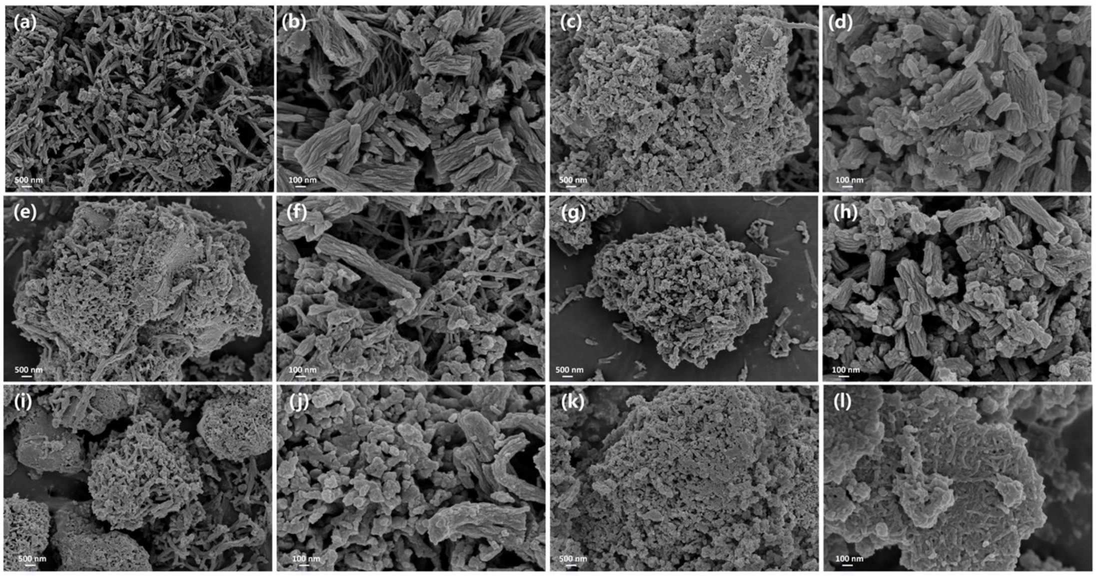

Fig. S2 SEM images of (Zr-MOF)$_x$/(TpTt-COF)$_y$,(a-b) x:y=3:7, (c-d) x:y=4:6, (e-f) x:y=5:5, (g-h) x:y=6:4, (i-j) x:y=7:3, (k-l) x:y=8:2

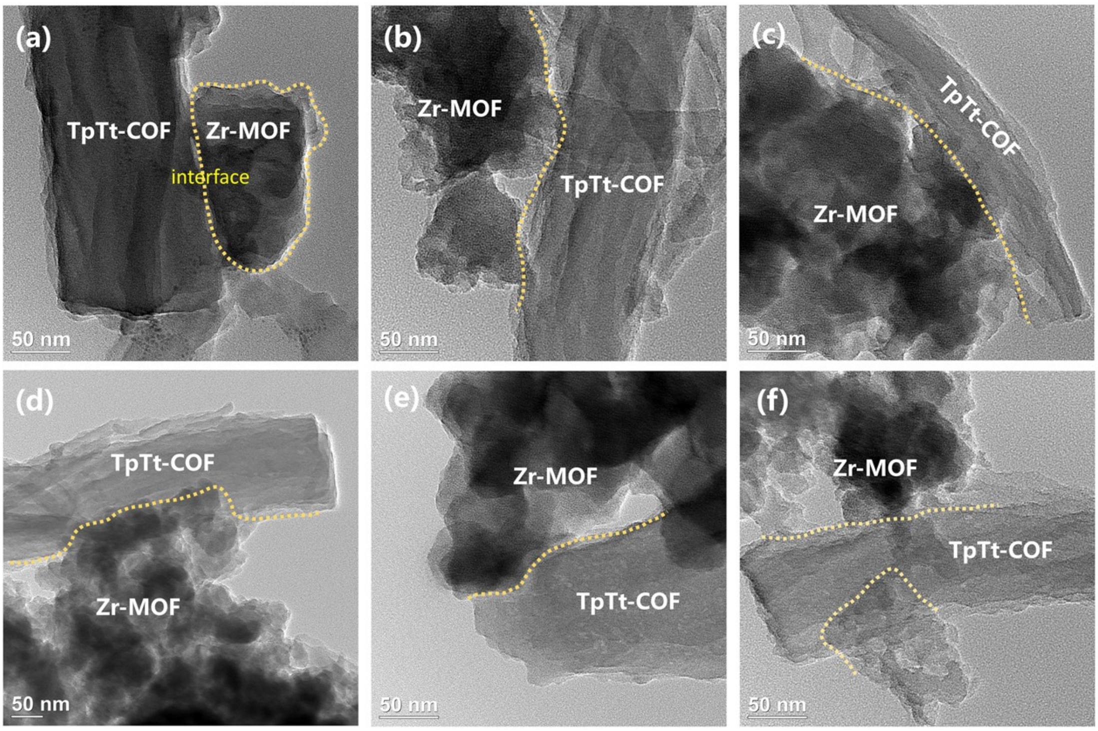

Fig. S3 HRTEM enlarged image of (Zr-MOF)$_x$/(TpTt-COF)$_y$,(a) x:y=3:7, (b) x:y=4:6, (c) x:y=5:5, (d) x:y=6:4, (e) x:y=7:3, (f) x:y=8:2

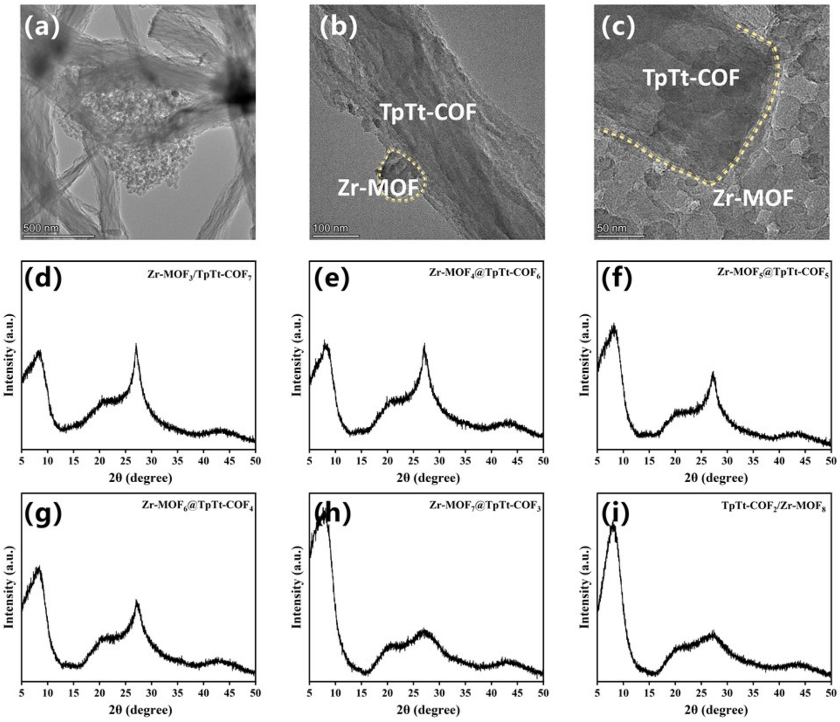

Fig. S4 HRTEM of (Zr-MOF)$_2$/(TpTt-COF)$_8$ (a-c) and XRD of (Zr-MOF)$_x$/(TpTt-COF)$_y$: (d) x:y=3:7, (e) x:y=4:6, (f) x:y=5:5, (g) x:y=6:4, (h) x:y=7:3, (i) x:y=8:2

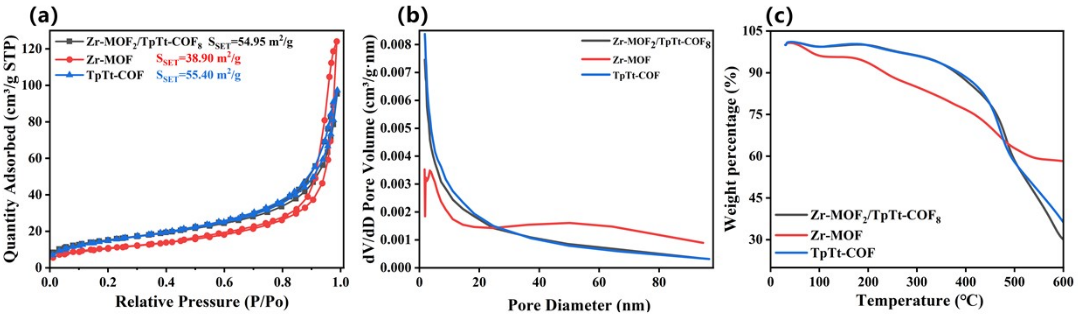

Fig. S5 (a) N_2 adsorption-desorption isotherms, (b) Pore size distribution and (c) Weight loss curves ofZr-MOF, TpTt-COF and $(Zr\text{-}MOF)_2/(TpTt\text{-}COF)_8$

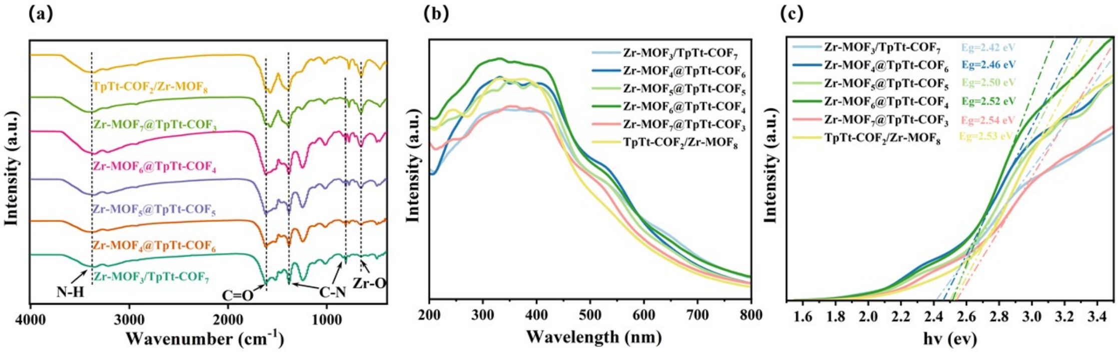

Fig. S6 (a) FT-IR spectra and (b) UV-Vis spectra of $(Zr\text{-}MOF)_x/(TpTt\text{-}COF)_y$ (x:y=3:7, 4:6, 5:5 6:4, 7:3, 8:2) (c) Tauc plots of $(Zr\text{-}MOF)_x/(TpTt\text{-}COF)_y$ (x:y=3:7, 4:6, 5:5 6:4, 7:3, 8:2)

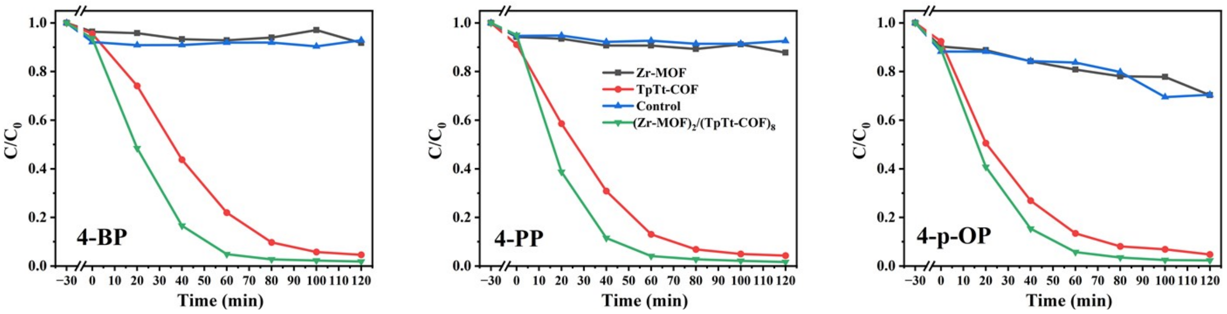

Fig. S7 Photocatalytic degradation of 4-BP, 4-PP and 4-p-OP under Zr-MOF, TpTt-COF, Control conditions and $Zr\text{-}MOF_2/TpTt\text{-}COF_8$

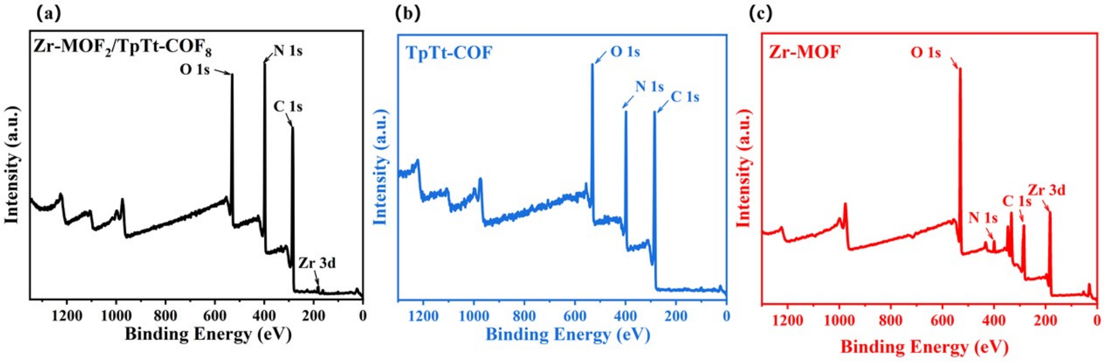

Fig. S8 XPS survey spectra of $(Zr\text{-}MOF)_2/(TpTt\text{-}COF)_8$, TpTt-COF, Zr-MOF

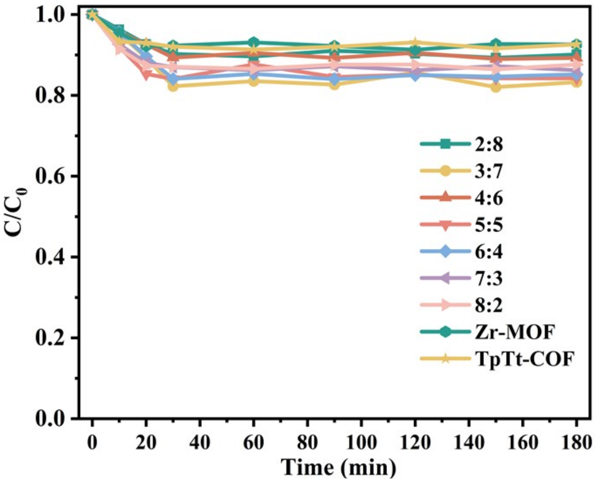

Fig. S9 Adsorption equilibrium curves of different photocatalysts

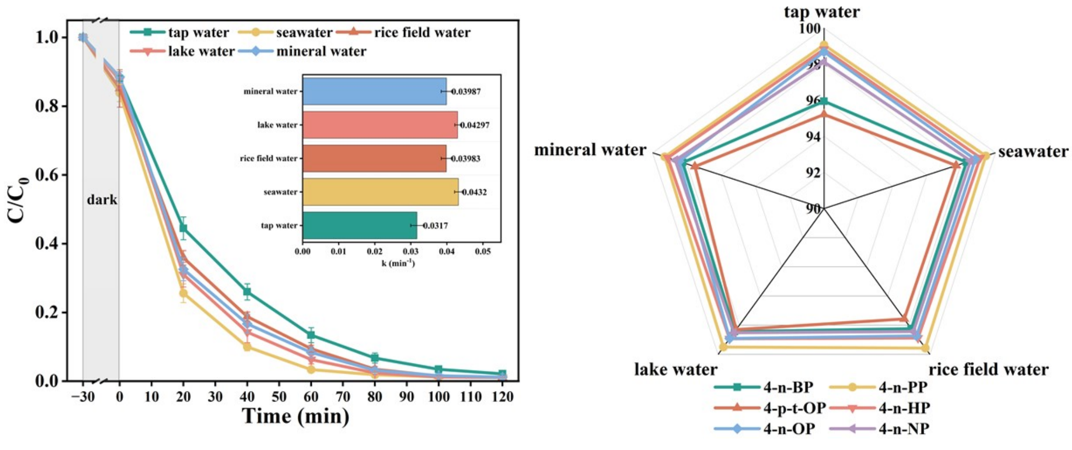

Fig. S10 Photocatalytic degradation trends of APs in different water bodies within 120 minutes (inset: photocatalytic rate) and removal efficiency of each AP at 120 min

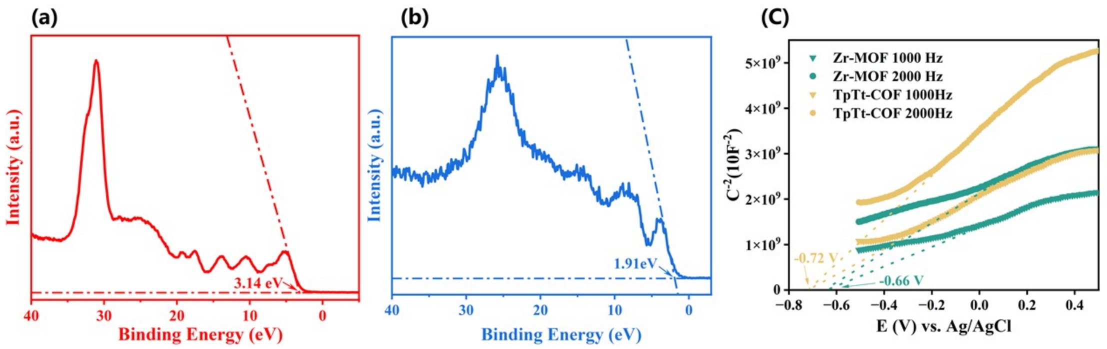

Fig. S11 XPS-VB of (a) Zr-MOF and (b) TpTt-COF; (c) Mott-Schottky plots of Zr-MOF and TpTt-COF

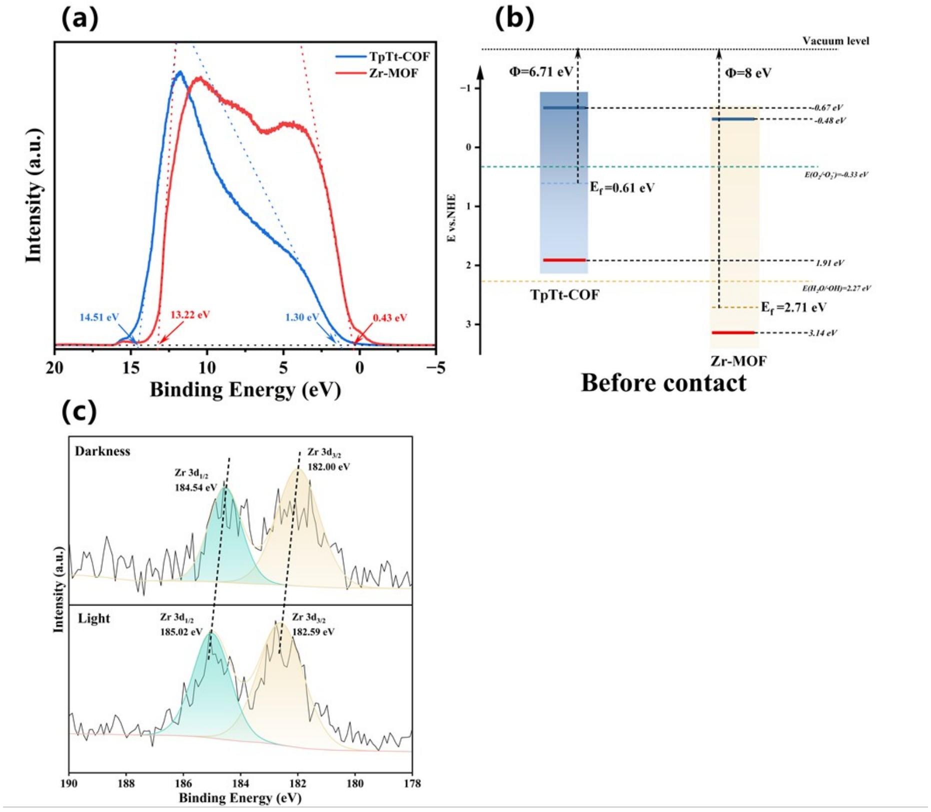

Fig. S12 (a) Ultraviolet photoelectron spectroscopy of TpTt-COF and Zr-MOF; (b) Energy level diagram of TpTt-COF and Zr-MOF

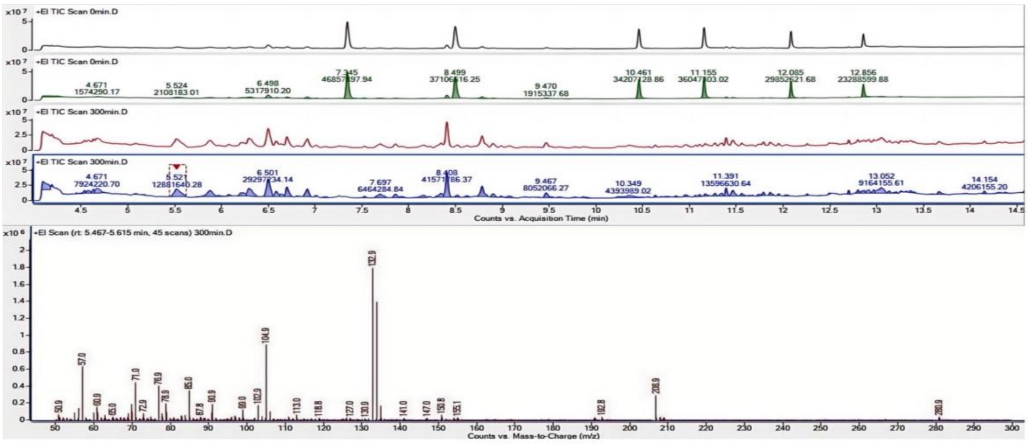

Fig. S13 the total ion chromatogram and mass spectrum of P1

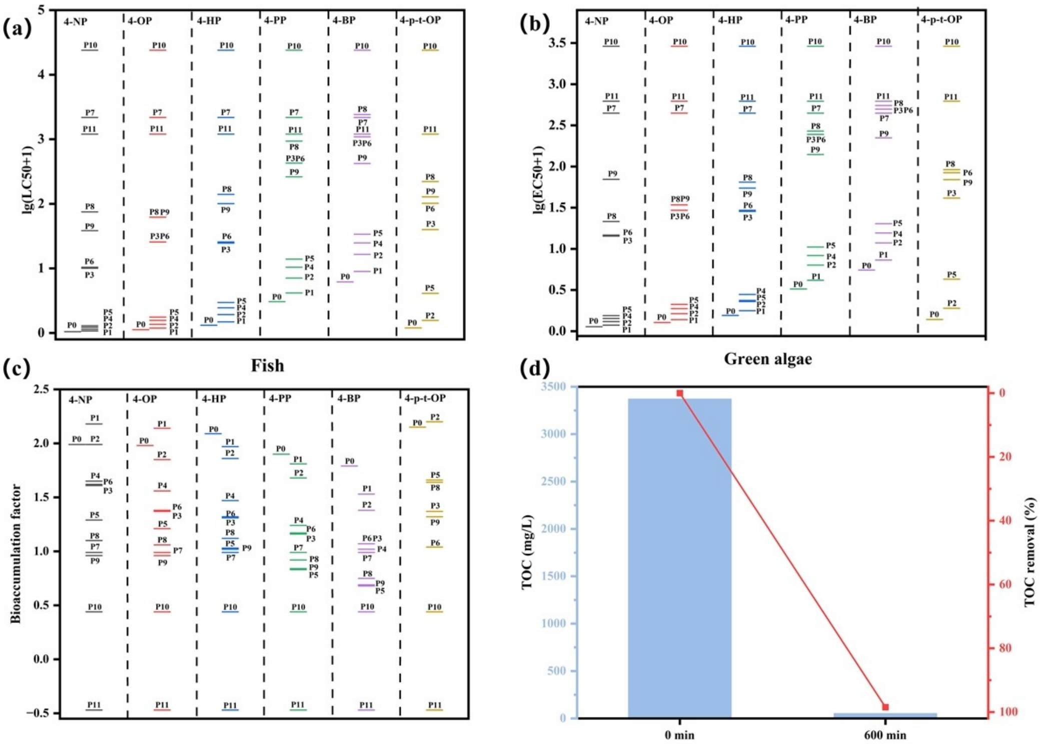

Fig. S14 (a) LC50 of APs on fish, (b) EC50 of APs on green algae, (c) Bioaccumulation factor of APs, (d) The organic carbon content and removal rate in 600 min

Table S1 Chromatography and mass parameters of GC-MS/MS

Model	Chromatography parameters	Mass parameters					
SIM	APs were separated on an HP-5 ms UI capillary column (0.25 mm i.d. × 30 m, 0.25 μm film thickness). The column was set at a constant flow rate of 1.2 mL/min, using helium as carrier gas. The oven temperature was programmed as follows: the initial temperature was 100 °C, held for 1 min, increased to 180 °C at 15 °C/min, held for 3 min, then ramped to 250 °C at 20 °C/min, held for 1 min; the total run time was 13.83 min. The injector temperature was 280 °C, and the injection volume was 1 μL in splitless mode. The ion source and transfer line temperatures were set to 280 °C.	APs	m/z^*	*m/z 1*	*m/z 2*	*m/z 3*	*RT*
		4-n-BP	150	77	107	108	7.34
		4-n-PP	107	164	108	77	8.50
		4-p-t-OP	135	206	107	136	10.46
		4-n-HP	192	107	108	77	11.15
		4-n-OP	206	107	108	77	12.09
		4-n-NP	220	107	135	108	12.86
Full scan	APs were separated on an HP-5 ms UI capillary column (0.25 mm i.d. × 30 m, 0.25 μm film thickness). The column was set at a constant flow rate of 1.2 mL/min, using helium as carrier gas. The oven temperature was programmed as follows: the initial temperature was 100 °C, held for 1 min, increased to 180 °C at 15 °C/min, held for 3 min, then ramped to 250 °C at 20 °C/min, held for 2 min; the total run time was 14.83 min. The injector temperature was 280 °C, and the injection volume was 1 μL in splitless mode. The ion source and transfer line temperatures were set to 280 °C.	Full scan range of *m/z*: 50-400					

Note: *m/z** Quantitative ion

m/z 1, m/z 2, m/z 3 Qualitative ion

Table S2 Comparison of alkylphenols degradation performance with other materials

Photocatalyst	Solution concentration	Catalyst mass	Solution volume	Catalyst concentration	Light Source	Reaction time （min）	Removal rate (%)	Types	Ref
$BiVO_4$	295.24 $mg·L^{-1}$	100 mg	20 mL	5 $mg·mL^{-1}$	visible light	Within 200 min	＞90	9	[2]
$Ag\text{-}BiVO_4$	295.24 $mg·L^{-1}$	200 mg	25 mL	8 $mg·mL^{-1}$	visible light	Within 200 min	＞50	9	[3]
TiO_2-Graphene	5 $mg·L^{-1}$	20 mg	200 mL	0.1 $mg·mL^{-1}$	UV lamp	180 min	50	3	[4]
TiO_2/CnTAB	8.25 $mg·L^{-1}$	5 mg	50 mL	0.1 $mg·mL^{-1}$	UV irradiation	120 min	＞95	3	[5]
$TiO_2/S_2O_8^{2-}$	10.31 $mg·L^{-1}$	28 cm^3	1000 mL	0.028 $cm^3·mL^{-1}$	UV	Within 200 min	＞95	1	[6]
$Zr\text{-}MOF_2/TpTt\text{-}COF_8$	6 $mg·L^{-1}$	5 mg	50 mL	0.1 $mg·mL^{-1}$	visible light	Within 120 min	＞98.2	6	This work

References

1 J. Wang, J. Qin, B. Liu and S. Song, Reaction mechanisms and toxicity evolution of Sulfamethoxazole degradation by CoFe-N doped C as Electro-Fenton cathode, *Sep. Purif. Technol.*, 2022, **298**, 121655.

2 S. Kohtani, M. Koshiko, A. Kudo, K. Tokumura, Y. Ishigaki, A. Toriba, K. Hayakawa and R. Nakagaki, Photodegradation of 4-alkylphenols using $BiVO_4$ photocatalyst under irradiation with visible light from a solar simulator, *Appl. Catal. B*, 2003, **46**(3), 573-586.

3 S. Kohtani, J. Hiro, N. Yamamoto, A. Kudo, K. Tokumura and R. Nakagaki, Adsorptive and photocatalytic properties of Ag-loaded $BiVO_4$ on the degradation of 4-n-alkylphenols under visible light irradiation, *Catal. Commun.*, 2005, **6**(3), 185-189.

4 C. Basheer, Application of titanium dioxide‐graphene composite material for photocatalytic degradation of alkylphenols, *J. Chem.*, 2013, **2013**(1), 456586.

5 T. Sakai, A. Da Loves, T. Okada and S. Mishima, Titania/CnTAB Nanoskeleton as adsorbent and photocatalyst for removal of alkylphenols dissolved in water, *J. Hazard. Mater.*, 2013, **248-249**, 487-495.

6 S. Yamazaki, T. Mori, T. Katou, M. Sugihara, A. Saeki and T. Tanimura, Photocatalytic degradation of 4-tert-octylphenol in water and the effect of peroxydisulfate as additives, *J. Photoch. Photobio. A Chem.*, 2008, **199**(2-3), 330-335.